Energy Reports 9 (2023) 165–170

Contents lists available at ScienceDirect

Energy Reports

journal homepage: www.elsevier.com/locate/egyr

Optimal planning of integrated energy system considering swapping station and carbon capture power system☆

Chenke He [a], Jizhong Zhu [a,*], Kwok Cheung [b], Alberto Borghetti [c], Di Zhang [a], Haohao Zhu [a]

[a] South China University of Technology, 381 Wushan Road, Tianhe District, Guangzhou 510641, China
[b] GE Digital, Bothell, WA 98011, USA
[c] University of Bologna, Bologna 40136, Italy

ARTICLE INFO

Keywords:
Planning
Integrated energy system (IES)
Swapping station (SS)
Carbon capture power system (CCPS)

ABSTRACT

An optimal planning method for an integrated energy system (IES) considering electric vehicles (EVs) swapping station (SS) and carbon capture power system (CCPS) is studied in this paper. Firstly, based on the analysis of swapping EV load, the model of SS is established. Then, we built the models of CCPS, and other energy supply and storage equipment in IES. Based on this, the annual comprehensive cost of planning is regarded as the optimization objective, a planning model of IES considering SS and CCPS is developed, and solved by CPLEX. Finally, an actual case was analyzed to verify the feasibility and effectiveness of the planning method proposed in this paper.

1. Introduction

Integrated energy system (IES) takes the grid as the core, coupling multiple energy sources, i.e., electricity, heating, cooling, and natural gas, and achieving efficient energy utilization via coordination and optimization of various energy production, transmission, storage, conversion, and distribution processes. Carbon capture power system (CCPS) can be an important technological choice for achieving low carbonization. Then, electric vehicles (EVs) swapping station (SS) is an EV centralized charging and swapping facility that integrates EV swapping and battery charging, with the advantages of high efficiency, energy saving, and low emissions. The comprehensive optimal planning of IES considering SS and CCPS will have a profound impact on the low-carbon planning and.

operating of future transportation and multi-energy integration system, which has important research significance.

One of the fundamental attributes of the Energy Internet, as outlined in the book "Third Industrial Revolution" by American scholar Rifkin, is its ability to support the electrification of transportation systems, and facilitate widespread access to EVs (Maier and Levesque., 2014). In this context, IES is an important physical carrier of the Energy Internet (Cheng et al., 2019). Considering the future integration of energy and transportation, there will be a growing interdependence between EV charging and swapping facilities and the planning and operation of IES (Shoja et al., 2022a; Wang et al., 2020a). Currently, there has been a notable growth of EV loads, leading to a heightened convergence between the regional terminal multi-energy supply system, specifically the IES integrating combined heat and power (CHP), and swapping stations that offer swapping services for EVs. In light of the growing emphasis on decarbonization efforts, an increasing number of CHP systems are being equipped with carbon capture systems (Chen et al., 2023a; Kumar et al., 2023). The adoption of carbon capture systems in CHP systems represents a proactive measure towards achieving decarbonization targets and promoting more sustainable energy practices. By integrating carbon capture systems into CHP systems, the aim is to mitigate and reduce carbon emissions. It is important to emphasize that the planning and operation of each individual link within this integrated system have a profound impact on the others. The rationality and accuracy of planning and operations in any given link have far-reaching implications for the entire system.

At present, there is no research on optimal planning of IES considering SS. As an EV centralized charging and swapping facility, the SS is also an important energy consumption terminal for IES. However, many scholars have studied IES with EVs or charging station. A scheduling method of a wind-photovoltaic-gas-EVs community-IES considering uncertainty and carbon emissions reduction is developed in (Zhu et al.,

☆ 2023 8th International Conference on Sustainable and Renewable Energy Engineering (ICSREE 2023) 11–13 May, Nice, France.

* Corresponding author.
E-mail address: zhujz@scut.edu.cn (J. Zhu).

https://doi.org/10.1016/j.egyr.2023.09.120
Received 30 August 2023; Accepted 20 September 2023
Available online 30 September 2023

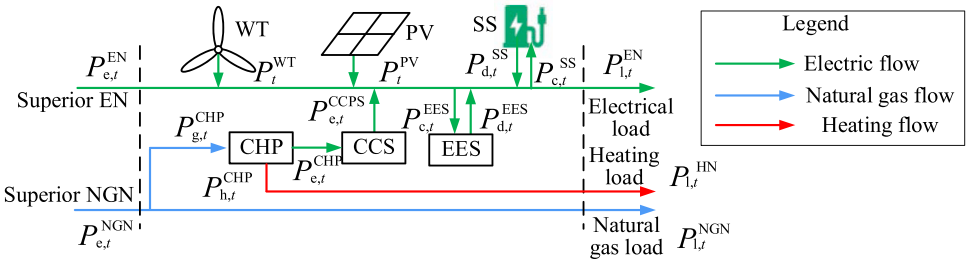

Fig. 1. Structure of IES considering SS and CCPS.

2023). In (Hai et al., 2023), a planning model of IES in a microgrid incorporating EVs is built. An energy supply strategy of EV charging parks and hydrogen refueling stations integrated into local IES is proposed in (Shoja et al., 2022b). In (Yang et al., 2022a), an optimal economic-emission planning model of IESs integrated EVs is established. A configuration model of multi-park IESs considering EV charging stations to assist services of shared energy storage power station is developed in (Jianwei et al., 2022). A Nash bargaining energy trading approach for an IES and EV charging stations is proposed in (Wang et al., 2020b). In (Rosato et al., 2017), the effects of EV charging on the performance of a residential building-integrated micro-trigeneration system are analyzed. Thus, the IES planning considering SS is needed to further research.

Currently, there are few studies on IES considering CCPS, and there is no study on comprehensive planning of IES considering CCPS and SS further. In (Chen et al., 2023b), an optimization method on an IES of combined heat and power, carbon capture system, and power-to-gas is proposed. An operation optimization model of IES considering power-to-gas technology and carbon capture system is developed in (Li et al., 2023). In (Wu and Li., 2023), an operation model of hydrogen-based IES with refined power-to-gas and carbon-capture-storage technologies under carbon trading is established. A low-carbon operation approach of IES based on carbon capture technology and carbon trading is designed in (Wang et al., 2022). In (Dong et al., 2022), a low-carbon planning model of an IES considering combined power-to-gas and carbon capture systems are built. A dispatch problem in IES considering multi-energy demand response and carbon capture technologies is solved in (Yang et al., 2022b). A model of combined heat and power with a power-to-gas and carbon capture system in IES is established in (Ma et al., 2021). In (Zhang and Zhang., 2020), an environment-friendly and economical scheduling approach for IES considering carbon capture power plants is developed. Therefore, the study on optimal planning of IES considering SS and CCPS is needed research.

Based on the above research background, the research content of this article is as follows: (1) Based on the modeling of charging and swapping systems, an optimal configuration model of SS is established; (2) According to the structure and operational characteristics of CCPS, build configuration model of CCPS, and then the models of other energy supply and storage equipment (ESSE) in IES are established; (3) We establish an optimal planning model of IES considering SS and CCPS, which regards the planning annual comprehensive cost as the optimization objective, and CPLEX is used to solve the model.

2. The framework of IES integrating swapping station and carbon capture power system

Firstly, we developed a framework of IES that incorporates two key components: the SS and the combined heat and power system with CCPS. Fig. 1 illustrates the framework of IES integrating SS and CCPS, which integrates electric network (EN), natural gas network (NGN) and heating network (HN) of IES. As the main energy supply devices in IES, the ESSE includes wind turbine (WT), photovoltaic (PV), CCPS, and SS. Furthermore, the EV loads in this region are serviced by the SS in IES.

3. Swapping station modeling

The establishment of the SS model serves as the basis for constructing the comprehensive planning model of the IES. By developing this sub-model, we lay the groundwork for the subsequent construction of the overall IES planning model. This sub-model provides focused and detailed models of specific components and their operations and configurations within the SS.

3.1. EV load analysis of SS

Except for different forms of energy supply (i.e., charging and swapping), the swapping EV (SEV) parameters (i.e., the capacity of EV, etc.) are the same as those of plug-in EVs. In addition, users' driving habits of SEVs are similar to plug-in EVs. There is no doubt that the initial swapping time of the SEV and the initial charging time of the plug-in EV can be regarded as the same. In other words, the probability distribution of the initial swapping time of SEV can be described as (1) (Gong et al., 2017). And (2) represents the probability distribution of the daily travel distances of SEVs (Gong et al., 2017).

$$f_S(t_0)=\begin{cases}1/\left(\sigma_S\sqrt{2\pi}\right)\exp\left[-(t_0-\mu_S)^2/\left(2\sigma_S^2\right)\right], & \mu_S-12<t_0\le 24\\ 1/\sigma_S\sqrt{2\pi}\exp\left[-(t_0+24-\mu_S)^2/\left(2\sigma_S^2\right)\right], & 0<t_0\le\mu_S-12\end{cases} \tag{1}$$

$$f_D(l)=1/\left(l\sigma_D\sqrt{2\pi}\right)\exp\left[-(\ln l-\mu_D)^2/\left(2\sigma_D^2\right)\right] \tag{2}$$

where μ_S and σ_S are the initial swapping time distribution parameters of the SEVs, and μ_S= 17.6, σ_S= 3.4, μ_D= 3.2, σ_D= 0.88.

3.2. SS modeling

The EV loads serve as a fundamental factor for the operation and configuration of the SS. Building upon the preceding analysis of the EV load within the SS, we develop a comprehensive SS model that takes into account both operational and configuration aspects. The structure of SS is shown in Fig. 2.

The SS model is constructed by (3)-(11). The power and state of charge (SOC) of SS are described in (3) and (4), respectively. (5) represents the number of high-level batteries in the SS needs to meet the EV loads. (6) and (7) give the charging and discharging power upper limits and power states of the battery charger. (8)-(10) calculates the number of swapping batteries, chargers, and swappers of the SS, respectively. The energy storage capacity of SS is given by (11).

$$P_t^{SS}=P_{c,t}^{SS}+P_{d,t}^{SS}=\sum_{i=1}^{N_{CH}}\left(P_{i,t}^{CH,c}+P_{i,t}^{CH,d}\right),\forall t \tag{3}$$

$$SOC_t^{SS} = SOC_{t-1}^{SS} + \left[\Delta t \sum_{i=1}^{N_{CH}} \left(\eta_c^{CH} P_{c,i,t-1}^{CH} - P_{d,i,t-1}^{CH} \Big/ \eta_d^{CH}\right) - \left(SOC_{max} - SOC_{min}\right) E_{SEV} N_{t-1}^{SEV}\right] / E_{SS}, \forall t \quad (4)$$

$$N_t^{SEV} \le N_{h,t}^{BA}, \forall t \quad (5)$$

$$0 \le P_{c,i,t}^{CH}, P_{d,i,t}^{CH} \le P_{max}^{CH}, \forall t \quad (6)$$

$$P_{c,i,t}^{CH} P_{d,i,t}^{CH} = 0, \forall t \quad (7)$$

$$\text{ceil}\left\{\left(1 + R_{BA}\right) N_{h,t}^{BA}\right\} \le N_{BA}, \forall t \quad (8)$$

$$\text{ceil}\{(1 + R_{CH}) N_{BA} / Z_{CH}\} \le N_{CH} \quad (9)$$

$$\text{ceil}\left\{\left(1 + R_{SW}\right) N_t^{SEV} / Z_{SW}\right\} \le N_{SW}, \forall t \quad (10)$$

$$E_{SS} = E_{SEV} N_{BA} \quad (11)$$

where, $P_{c,t}^{SS}$ and $P_{d,t}^{SS}$ are the charging and discharging powers of the SS, respectively. $P_{c,i,t}^{CH}$ and $P_{d,i,t}^{CH}$ are the charging and discharging powers of the charger, respectively. R_{SW}, R_{BA} and R_{CH} are the margin coefficients of the swappers, swapping energy storage, and chargers, respectively. $N_{h,t}^{BA}$ is the number of SS high-level batteries. N_{CH} and N_{SW} are the numbers of chargers and swappers, respectively. Z_{CH} and Z_{SW} the number of batteries simultaneously charged by a charger, and the number of SEVs simultaneously serviced by a swapper, respectively. E_{SEV} is the capacity of the SEV battery. N_{BA} and E_{SS} are the numbers of SS battery swapping and the swapping energy storage capacity of SS, respectively. P_{max}^{CH} is the upper limit of the charging and discharging powers of the charger, respectively. N_t^{SEV} is the number of SEV loads of the SS at time t. SOC_{max} and SOC_{min} are the upper and lower limits of energy storage SOC, respectively.

4. Modeling of IES

In the preceding chapter, we successfully constructed a sub-model, specifically the SS, as part of the planning model within the IES integrating SS and CCPS. Building upon this achievement, the focus of the current chapter is to develop another sub-model within the IES framework. Specifically, this chapter will encompass the modeling of various types of ESSE, including the CCPS. By incorporating these sub-models into the broader IES framework, we aim to create a comprehensive planning model that considers both the SS and the ESSE.

4.1. Modeling of carbon capture power system

The structure of carbon capture system (CCS) is shown in Fig. 3.

The model of CCPS based on a CHP and CCS is given by (12)-(17). The power outputs of the CCPS and CHP can be calculated by (12) - (14), respectively. And (15) restrain the CHP ramp constraint and the CCS power load, respectively. The equivalent power of the volume of CO_2 absorbed by the CCS is calculated by (16) and (17).

$$P_{e,t}^{CCPS} = P_{e,t}^{CHP} - P_t^{CCS}, \forall t \quad (12)$$

$$P_{e,t}^{CHP} = \eta_e^{CHP} P_{g,t}^{CHP}, \ P_{e,\,min}^{CHP} \le P_{e,t}^{CHP} \le P_{e,\,max}^{CHP}, \forall t \quad (13)$$

$$P_{h,t}^{CHP} = \eta_h^{CHP} P_{g,t}^{CHP}, \ P_{h,\,min}^{CHP} \le P_{h,t}^{CHP} \le P_{h,\,max}^{CHP}, \forall t \quad (14)$$

$$-\Delta P_{e,d}^{CHP} \le P_{e,t}^{CHP} - P_{e,t-1}^{CHP} \le \Delta P_{e,u}^{CHP}, \forall t \quad (15)$$

$$P_{a,t}^{CCS} = \alpha_{CO_2} P_t^{CCS}, \forall t \quad (16)$$

$$0 \le P_{a,t}^{CCS} \le P_{e,t}^{CHP}, \forall t \quad (17)$$

where $P_{e,t}^{CCPS}$ and $P_{e,t}^{CHP}$ are the electrical outputs of CCPS and CHP at time t, respectively. P_t^{CCS} is the energy consumption power of CCS at time t. $P_{e,max}^{CHP}$ and $P_{e,min}^{CHP}$ are the upper and lower limits of CHP electrical power output at time t, respectively. η_e^{CHP} and η_h^{CHP} are the CHP electrical and

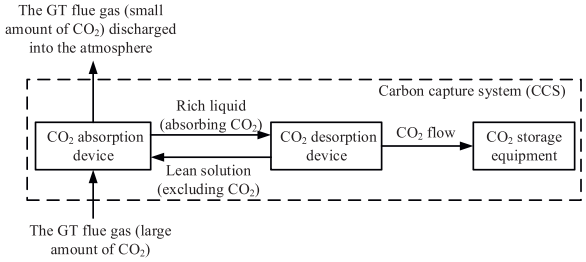

Fig. 3. Structure of CCS.

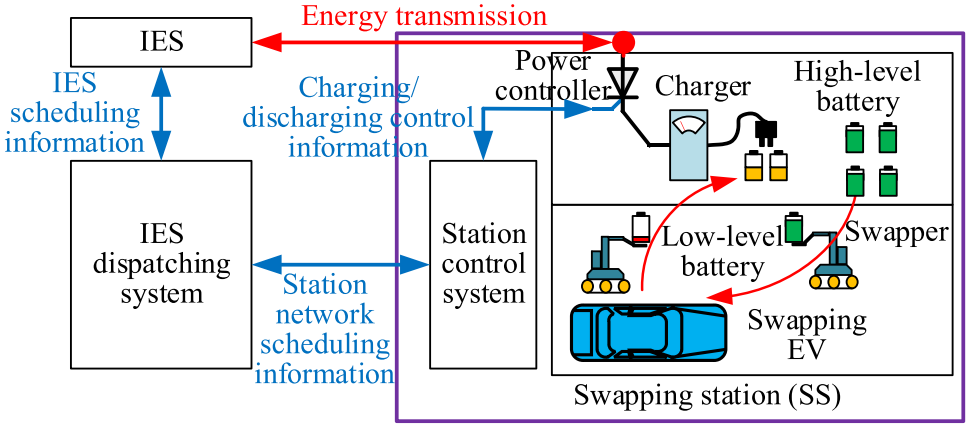

Fig. 2. Structure of SS.

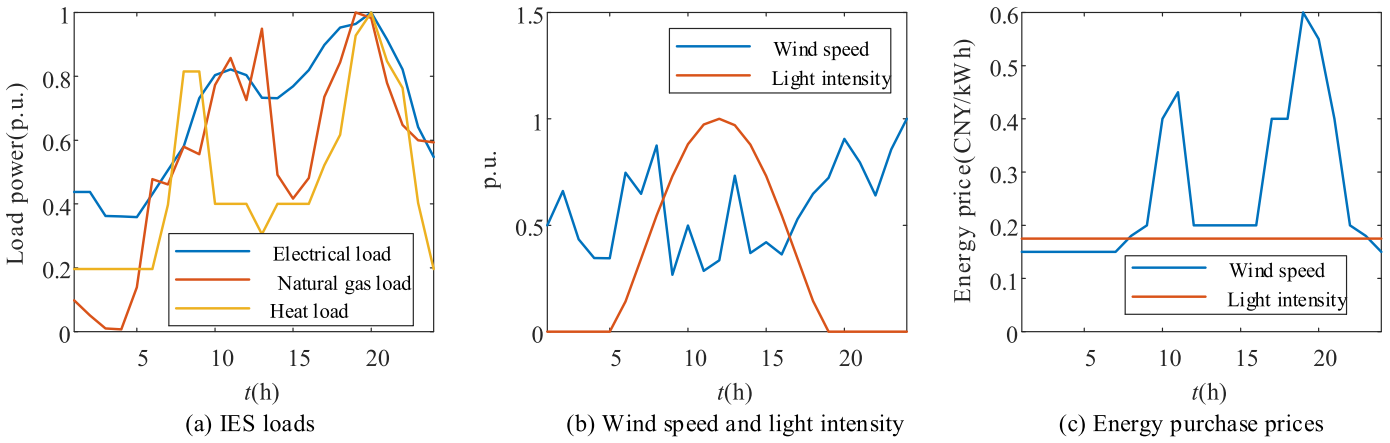

Fig. 4. Load, wind speed, light intensity, energy purchase prices of IES.

Table 1
Case study parameters I.

Parameter	Value	Parameter	Value	Parameter	Value
$R_{SW}/R_{BA}/R_{CH}$	0.2/0.2/0.2	E_{SEV}(kWh)	50	Z_{CH}/Z_{SW}	4/6
P_{max}^{CH}(kW)	50	SOC_{max}/SOC_{min}	0.95/0.2	$P_{h,max}^{CHP}/P_{h,min}^{CHP}$(kW)	1000/500
$W_{in}/W_{out}/W_n$(m/s)	3/25/14	$S_{min}^{WT}/S_{max}^{WT}$(kW)	500/2000	$\cos\phi_{DG}$	0.9
δ	0.06	$S_{min}^{PV}/S_{max}^{PV}$(kW)	500/2000	$\Delta P_{e,d}^{CHP}/\Delta P_{e,u}^{CHP}$(kW)	250/250
$P_{e,max}^{CHP}/P_{e,min}^{CHP}$(kW)	1000/500	D(days)	365	c_C(10^4CNY/kWh)	0.001

heating efficiencies, respectively. $P_{h,max}^{CHP}$ and $P_{h,min}^{CHP}$ are the upper and lower limits of CHP heating power output at time t, respectively. $\Delta P_{e,d}^{CHP}$ and $\Delta P_{e,u}^{CHP}$ are the up-down climbing rates, respectively. α_{CO_2} is the CO_2 absorption efficiency. $P_{a,t}^{CCS}$ is the equivalent power of the volume of CO_2 absorbed by the CCS at time t.

4.2. Modeling of wind turbine

The model of the wind turbine (WT) is given by (18)-(19): (18) represents the installed capacity of the WT is greater than the power output upper limit. (19) gives the WT power output.

$$P_t^{WT,c}/\cos\phi_{DG} \le S_{WT}, S_{min}^{WT} \le S_{WT} \le S_{max}^{WT}, \forall t \tag{18}$$

$$0 \le P_t^{WT} \le P_t^{WT,c}, P_t^{WT,c} = \begin{cases} 0 & , W(t) \le W_{out} \text{ or } W_t \ge W_{in} \\ P_n^{WT}(W_t - W_{in})/(W_n - W_{in}), & W_{in} \le W_t \le W_n, \forall t \\ P_n^{WT} & , W_n < W_t < W_{out} \end{cases} \tag{19}$$

where P_t^{WT} and $P_t^{WT,c}$ are the actual output of WT and the upper limit at time t, respectively. P_n^{WT} is the WT-rated power. W_t is the wind speed at time t. W_{in}, W_{out} and W_n are cut-in, cut-out, and rated wind speeds of WT, respectively. S_{WT}, S_{max}^{WT} and S_{min}^{WT} are the WT installed capacity and capacity upper and lower limits, respectively. $\cos\phi_{DG}$ is the DG power factor.

4.3. Modeling of photovoltaic

The installed capacity of photovoltaic (PV) is greater than its upper output limit. And (20) to (21) give the installed capacity and operating models, respectively.

$$P_t^{PV,c}/\cos\phi_{DG} \le S_{PV}, S_{min}^{PV} \le S_{PV} \le S_{max}^{PV} \forall t \tag{20}$$

$$0 \le P_t^{PV} \le P_t^{PV,c}, P_t^{PV,c} = R_t S_{PV}, \forall t \tag{21}$$

where, P_t^{PV} and $P_t^{PV,c}$ are the actual output of PV and its upper limit at time t, respectively. R_t is the unit value of light intensity at time t. S_{PV}, S_{max}^{PV} and S_{min}^{PV} are the PV installed capacity and capacity upper and lower limits, respectively.

5. Planning model IES considering SS and CCPS

By constructing the aforementioned sub-models and integrating them into the overall IES, we have successfully established an IES optimization planning model that takes into account the SS and CCPS. This optimization planning model enables us to analyze and optimize the entire IES system considering the SS and CCPS.

5.1. Objective

To minimize the planning annual comprehensive cost as the optimization objective, we establish the optimal planning model of IES considering SS and CCPS. The objective is as follows.

$$\min F = C_I + C_E + C_O + C_C \tag{22}$$

where, C_I, C_E, C_O and C_C are the costs of infrastructure, energy purchasing, operation-maintenance, and carbon trading of IES, respectively, which are calculated by (23)-(26).

$$C_I = \frac{\delta(1+\delta)^{Y_i}}{(1+\delta)^{Y_i}-1} \sum_{i \in ESSE} c_i^{ESSE} S_i^{ESSE} \tag{23}$$

$$C_E = D \sum_{t=1}^{T} \left(c_t^{EN,e} P_t^{EN,e} + c_t^{NGN,e} P_t^{NGN,e} \right) \tag{24}$$

$$C_O = \sum_{i \in ESSE} \left[\varphi_i^{ESSE,s} S_i^{ESSE} + D \sum_{t=1}^{T} \left(\varphi_i^{ESSE,o} \left| P_{i,t}^{ESSE} \right| \right) \right] \tag{25}$$

Table 2
Case study parameters II.

ESSE type	WT	PV	CHP	CCS	Charger	Swapper	Swapping battery
Unit capacity price	0.3(10^4CNY/kW)	0.5(10^4CNY/kW)	1.5(10^4CNY/kWh)	1(10^4CNY/kWh)	20(10^4CNY)	25(10^4CNY)	0.2(10^4CNY/kWh)
Service life (years)	20	20	20	20	20	20	10
Operational efficiency	—	—	0.4	0.9	0.9	—	0.9
Unit capacity annual operation-maintenance cost (10^3 CNY/year)	0.01	0.02	0.1	0.1	0.05	0.01	0.005
Unit operating power operation-maintenance cost (CNY/kWh)	0.05	0.03	0.5	0.5	—	—	0.1
Unit capacity	250(kW)	250(kW)	250(kW)	250(kW)	—	—	50(kW)

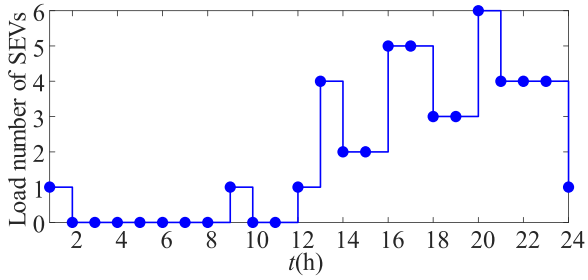

Fig. 5. EV loads of the service area.

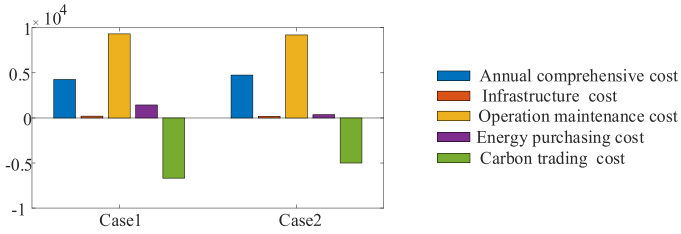

Fig. 6. Optimal results of planning economy.

$$C_{\mathrm{C}}=\frac{D\Delta t c_{\mathrm{C}}}{1000}\sum_{t=1}^{T}\sum_{\substack{i\in ESSE,\\ i\notin DG,i\notin CCS}}\left[\left(1-\lambda_i^{\mathrm{ESSE}}\right)\left|P_{i,t}^{\mathrm{ESSE}}\right|-P_t^{\mathrm{WT}}-P_t^{\mathrm{PV}}-P_{\mathrm{a},t}^{\mathrm{CCS}}\right]-E_{\mathrm{ba}}^{\mathrm{C}} \tag{26}$$

where, S_i^{ESSE}, c_i^{ESSE} and Y_i are the configured capacity, unit capacity price, and service life of the type i ESSE, respectively. δ is the discount rate. D is the number of days per year. $P_t^{\mathrm{EN,e}}$ and $c_t^{\mathrm{EN,e}}$ are the interactive power between IES and the superior electric system, and the unit electricity purchase price of IES, respectively. $P_t^{\mathrm{NGN,e}}$ and $c_t^{\mathrm{NGN,e}}$ are the interactive power between IES and the superior natural gas system, and the unit natural gas purchase price of IES, respectively. $\varphi_i^{\mathrm{ESSE},s}$and $\varphi_i^{\mathrm{ESSE},o}$ are the annual operation-maintenance costs of unit capacity and unit operating power of the type i ESSE, respectively. $P_{i,t}^{\mathrm{ESSE}}$ is the operating power of the type i ESSE. *ESSE*, *DG*, and *CCS* are equipment sets of ESSE, DG, and CCS, respectively. $\lambda_i^{\mathrm{ESSE}}$ is the operational efficiency of the type i ESSE. c_C is the carbon trading cost per unit energy. E_{ba}^{C} is the basic carbon quota of IES (equivalent energy).

Table 3
Optimal configuration results of system.

ESSE type	Case1	Case2
WT (kW)	1000	1000
PV (kW)	1000	1000
CHP (kW)	500	500
CCS (kW)	400	300
Charger	3	3
Swapper	5	5
Swapping battery (kWh)	400	400

5.2. Constraints

- Equipment capacity constraints. Due to configuration conditions i.e., equipment occupation, etc., (27) gives the capacity limit constraints of candidate equipment of IES.

$$0\le S_i^{\mathrm{ESSE}}\le S_{i,\ \max}^{\mathrm{ESSE}},\ i\in ESSE \tag{27}$$

  where, $S_{i,\max}^{\mathrm{ESSE}}$ is the maximum configuration capacity of the type i ESSE.
- Energy balance constraints.

$$P_{\mathrm{e},t}^{\mathrm{EN}}+P_{\mathrm{e},t}^{\mathrm{CCPS}}+P_t^{\mathrm{WT}}+P_t^{\mathrm{PV}}+P_{\mathrm{d},t}^{\mathrm{SS}}=P_{\mathrm{c},t}^{\mathrm{SS}}+P_{\mathrm{l},t}^{\mathrm{EN}},\forall t \tag{28}$$

$$P_{\mathrm{e},t}^{\mathrm{NGN}}=P_{\mathrm{g},t}^{\mathrm{GT}}+P_{\mathrm{l},t}^{\mathrm{NGN}},\forall t \tag{29}$$

$$P_{\mathrm{h},t}^{\mathrm{CHP}}=P_{\mathrm{h},t}^{\mathrm{HN}},\forall t \tag{30}$$

where, $P_{\mathrm{l},t}^{\mathrm{EN}}$, $P_{l,t}^{\mathrm{NGN}}$, and $P_{h,t}^{\mathrm{HN}}$ are the EN, NGN and HN loads, respectively.

6. Case study

6.1. Parameter settings

The structure of the IES is visualized in Fig. 1. The basic load curve and the unit purchase energy prices of IES, wind speed, and light intensity are shown in Fig. 4. The other parameters of IES are shown in Tables 1 and 2. Then, the CPLEX is used to solve the planning model developed in this paper.

This paper sets up two Cases to compare and study the planning methods developed: (1) Case1: SS participates in vehicle-to-grid (V2G) (Zhu et al., 2023) (i.e., charging and discharging powers of SS are flexible) to adjust IES; (2) Case2: the charging power of SS only to meet the load demands of EVs.

6.2. Case study analysis

Fig. 5 shows the EV loads of the service area.

The optimal results of planning economy are shown in Fig. 6. The optimal configuration results of system are shown in Table 3. The annual comprehensive cost of Case 1 is the lowest, and the annual comprehensive cost of Case 1 is 482.26 × 10^4 CNY lower than that of Case 2. This indicates that Case1 has the best economy. In terms of costs of infrastructure, operation-maintenance, and energy purchasing, Case 1 is 8.72 × 10^4 CNY, 110.32 × 10^4 CNY, and 1084.29 × 10^4 CNY higher than Case 2, respectively. Then, due to the V2G participation of Case 1′s SS, which achieved the regulation of IES and assisted carbon reduction, the carbon cost of Case 1 is 1685.59 × 10^4 CNY lower than that of Case 2. In addition, due to the participation of Case 1′s SS in V2G and IES for

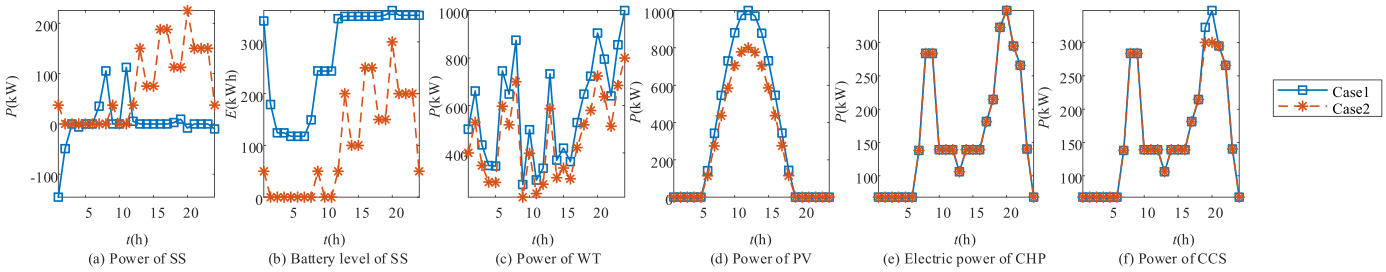

Fig. 7. Optimal operating status of system.

carbon reduction, the system's operational flexibility has been improved. Therefore, the CCS configuration capacity of Case 1 is higher than that of Case 2.

The optimal operating status of system is shown in Fig. 7. Due to the participation of SS in V2G regulation of IES in Case1, SS can flexibly charge and discharge to regulate IES, while Case2 has a smaller regulatory ability. So, the power outputs of WT, PV, and CCS (i.e., clean energy) in Case1 is higher than that in Case2. Besides, the operating power of Case1 and Case2 can meet the load demands of SEVs.

7. Conclusion

This paper develops an optimal planning method of IES considering SS and CCPS. The conclusion is as follows:

1) Compared to cases of SS does not participate in V2G, the planning case of SS that participates in V2G has the lowest annual comprehensive cost of IES, and has the best carbon trading costs, which has the best comprehensive economy and environmental protection.
2) Compared to cases of SS does not participate in V2G, SS that can flexibly charge and discharge (i.e., participate in V2G) has the best operational coordination and complementarity with CCPS, has better energy storage regulation ability, and can better leverage the carbon reduction effect of CCPS in IES.

The method proposed in this paper is feasible and effective for solving the optimal planning problem of IES considering SS and CCPS, and provides a certain theoretical basis for the comprehensive planning of future transportation and multi energy integrated system.

Declaration of Competing Interest

The authors declare no conflict of interest.

Data availability

Data will be made available on request.

Acknowledgements

This work was supported by the National Natural Science Foundation of China (52177087) and the High-end Foreign Experts Project (G2022163018L).

References

Chen, Maozhi, Lu, Hao, Chang, Xiqiang, Liao, Haiyan, 2023a. An optimization on an integrated energy system of combined heat and power, carbon capture system and power to gas by considering flexible load. Energy 273 (2023), 127203.
Chen, Maozhi, Lu, Hao, Chang, Xiqiang, Liao, Haiyan, 2023b. An optimization on an integrated energy system of combined heat and power, carbon capture system and power to gas by considering flexible load. Energy 273 (2023), 127203.
Cheng, Lefeng, Yu, Tao, Jiang, Haorong, Shi, Shouyuan, Tan, Zhukui, Zhang, Zhiyi, 2019. Energy internet access equipment integrating cyber-physical systems: concepts, key technologies, system development, and application prospects. IEEE Access 7 (2019), 23127–23148.
Dong, Wenkai, Lu, Zhigang, He, Liangce, Geng, Lijun, Guo, Xiaoqiang, Zhang, Jiangfeng, 2022. Low-carbon optimal planning of an integrated energy station considering combined power-to-gas and gas-fired units equipped with carbon capture systems. Int. J. Electr. Power Energy Syst. 138 (2022), 107966.
Gong Lili Cao Wu Zhao Jianfeng. Load modeling method for EV charging stations based on trip chain 2017 IEEE Conference on Energy Internet and Energy System *Integration (EI2)*, Beijing, China 2017.
Hai, Tao, Zhou, Jincheng, khaki, Mehrdad, 2023. Optimal planning and design of integrated energy systems in a microgrid incorporating electric vehicles and fuel cell system. J. Power Sources 561 (2023), 232694.
Jianwei, Gao, Fangjie, Gao, Yu, Yang, Haoyu, Wu, Yi, Zhang, Pengcheng, Liang, 2022. Configuration optimization and benefit allocation model of multi-park integrated energy systems considering electric vehicle charging station to assist services of shared energy storage power station. J. Clean. Prod. 336 (2022), 130381.
Kumar, Tharun Roshan, Beiron, Johanna, Biermann, Maximilian, Harvey, Simon, Thunman, Henrik, 2023. Plant and system-level performance of combined heat and power plants equipped with different carbon capture technologies. Applied Energy 338 (2023), 120927.
Li, Xin, Li, Texun, Liu, Li, Wang, Zhen, Li, Xinyu, Huang, Jianan, Huang, Jingqi, Guo, Pangfeng, Xiong, Wei, 2023. Operation optimization for integrated energy system based on hybrid CSP-CHP considering power-to-gas technology and carbon capture system. J. Clean. Prod. 391 (2023), 136119.
Ma, Yiming, Wang, Haixin, Hong, Feng, Yang, Junyou, Chen, Zhe, Cui, Haoqian, Feng, Jiawei, 2021. Modeling and optimization of combined heat and power with power-to-gas and carbon capture system in integrated energy system. Energy 236 (2021), 121392.
Maier, Martin, Levesque, Martin, 2014. Dependable fiber-wireless (FIWI) access networks and their role in a sustainable third industrial revolution economy. IEEE Trans. Reliability 63 (2), 386–400 (2014).
Rosato, Antonio, Sibilio, Sergio, Ciampi, Giovanni, Entchev, Evgueniy, Ribberink, Hajo, 2017. Energy, environmental and economic effects of electric vehicle charging on the performance of a residential building-integrated micro-trigeneration system. Energy Procedia 111 (2017), 699–709.
Shoja, Zahra Moshaver, Mirzaei, Mohammad Amin, Seyedi, Heresh, Zare, Kazem, 2022a. Sustainable energy supply of electric vehicle charging parks and hydrogen refueling stations integrated in local energy systems under a risk-averse optimization strategy. J. Energy Storage 55 (2022), 105633.
Shoja, Zahra Moshaver, Mirzaei, Mohammad Amin, Seyedi, Heresh, Zare, Kazem, 2022b. Sustainable energy supply of electric vehicle charging parks and hydrogen refueling stations integrated in local energy systems under a risk-averse optimization strategy. J. Energy Storage 55 (2022), 105633.
Wang, Rutian, Wen, Xiangyun, Wang, Xiuyun, Fu, Yanbo, Zhang, Yu, 2022. Low carbon optimal operation of integrated energy system based on carbon capture technology, LCA carbon emissions and ladder-type carbon trading. Applied Energy 311 (2022), 118664.
Wang, Yifei, Wang, Xiuli, Shao, Chengcheng, Gong, Naiwei, 2020a. Distributed energy trading for an integrated energy system and electric vehicle charging stations: a nash bargaining. Renew. Energy 155 (2020), 513–530.
Wang, Yifei, Wang, Xiuli, Shao, Chengcheng, Gong, Naiwei, 2020b. Distributed energy trading for an integrated energy system and electric vehicle charging stations: a nash bargaining game approach. Renew. Energy 155 (2020), 513–530.
Wu, Qunli, Li, Chunxiang, 2023. Modeling and operation optimization of hydrogen-based integrated energy system with refined power-to-gas and carbon-capture-storage technologies under carbon trading. Energy 270 (2023), 126832.
Yang, Dongfeng, Xu, Yang, Liu, Xiaojun, Jiang, Chao, Nie, Fanjie, Ran, Zixu, 2022b. Economic-emission dispatch problem in integrated electricity and heat system considering multi-energy demand response and carbon capture technologies. Energy 253 (2022), 124153.
Yang, Wenjun, Guo, Jia, Vartosh, Aris, 2022a. Optimal economic-emission planning of multi-energy systems integrated electric vehicles with modified group search optimization. Applied Energy 311 (2022), 118634.
Zhang, Xingping, Zhang, Youzhong, 2020. Environment-friendly and economical scheduling optimization for integrated energy system considering power-to-gas technology and carbon capture power plant. J. Clean. Prod. 276 (2020), 123348.
Zhu, Gang, Gao, Yan, Sun, Hao, 2023. Optimization scheduling of a wind–photovoltaic–gas–electric vehicles community-integrated energy system considering uncertainty and carbon emissions reduction. Sustain. Energy Grids Netw. 33 (2023), 100973.